Theor Chem Acc (2007) 118:271–279
DOI 10.1007/s00214-007-0319-1

REGULAR ARTICLE

Ab initio DFT study of Z–E isomerization pathways of *N*–benzylideneaniline

Alexander V. Gaenko · Ajitha Devarajan · Laura Gagliardi · Roland Lindh · Giorgio Orlandi

Received: 22 November 2006 / Accepted: 5 April 2007 / Published online: 26 May 2007

Abstract The ground state properties and absorption spectra of *N*-benzylideneaniline (NBA) have been studied at the density functional (DFT) and at the time-dependent density functional (TD-DFT) level of the theory. The equilibrium geometries of the E and Z isomers in the ground state and their vibrational frequencies have been computed. Furthermore, the excitation energies of the lowest excited singlet and triplet states and the potential energy curves along the torsion and the inversion isomerization coordinates were evaluated. The results are discussed in light of the available experimental data.

1 Introduction

N-benzylideneaniline (NBA) belongs to the family of compounds containing the –CH=N– double bond, which are of interest in many fields of chemistry and biochemistry [1–5]. The photochemistry of the –CH=N– double bond has been extensively studied in the past [4]. The azomethine group present in rhodopsin plays a central role in the light-driven proton pump process occurring during visual cycle [1–3]. Furthermore, NBA and its derivatives are currently investigated as molecules with promising non-linear optical properties on account of possible applications in the field of photonics [5].

NBA is an azomethine that is structurally similar and is isoelectronic with stilbene (CH=CH bond) and azobenzene (N=N bond). In spite of this, the ultraviolet spectrum of NBA is remarkably different from the spectra of azobenzene and stilbene [6,7]. According to experimental [8,9] and theoretical studies [10–12] the main reason for this difference is the non-planar conformation of NBA, which is caused by the conjugation between the aniline ring and the nitrogen lone pair. This is in contrast to the nearly planar structure of the two other isoelectronic molecular systems. The structure and the main geometric parameters of NBA are shown in Fig. 1.

The non-planarity of NBA is associated with non-zero values of two parameters that define the molecular conformation: the torsion angle (α) about the N-phenyl bond, which has been found to be 55° in the solid [9] and 52° in the gas phase by electron diffraction [13], and the C_7–C_2 torsion (β), which is 10.3° [9] in the solid and is assumed to be zero in the gas phase. A Hartree–Fock study indicated that the non-planar conformation, associated with $\alpha = 45°$ and $\beta = 0°$, is favoured over the planar one by 6.58 kJ/mol [11]. Since this energy difference is relatively small, the molecular conformation may be altered by small perturbations such as atom substitutions or by the intermolecular interactions provided by a solid phase.

The relation between the non-planar structure and the spectral shape of NBA was supported by the finding that the diffuse reflectance spectrum of NBA in the solid phase, where

A. V. Gaenko
St-Petersburg State Institute of Technology (Technical University), Moskovskii av. 26, 198013, St-Petersburg, Russia

A. Devarajan (✉)
Chemistry Department, University of North Dakota, P. O. Box 9024, Grand Forks, ND 58201-9024, USA
e-mail: adevarajan@mail.chem.und.nodak.edu

L. Gagliardi
Department of Physical Chemistry, Sciences II, University of Geneva, 1211 Geneva 4, Switzerland

R. Lindh
Chemical Physics Department, Chemical Center, Lund University, P. O. Box 124, 221 00 Lund, Sweden

G. Orlandi
Department of Chemistry "G. Ciamician", University of Bologna, 40126 Bologna, Italy

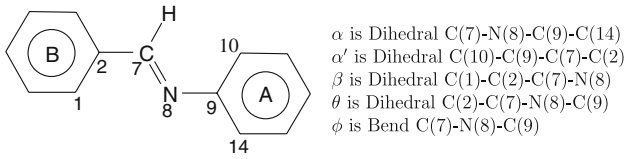

Fig. 1 Molecular structure and most relevant structural parameters of *N*-benzylideneaniline

the molecule is known to be non-planar, is similar to the spectrum observed in solution [14]. On the contrary, the absorption spectrum of di-chloro-benzylideneanilne (DCBA) in the triclinic crystalline polymorph [15], where it is known to take a planar conformation, resembles the spectra of azobenzene and stilbene. This observation provided the direct proof that the non-planar structure is the cause responsible for the peculiar spectrum of NBA in solution.

The study of E–Z photoisomerization of di-aryl compounds R–CH=CH–R ′, R–N=N–R′ and R–N=CH–R′, where R and R′ are aryls, can be useful to tailor molecular devices, based on reversible photochemical reactions, that respond in the desired way to external stimuli. While stilbene isomerizes only by internal rotation about the CH=CH bond, azobenzene and benzylideneaniline may isomerize by N=N or CH=N bond torsion (θ) and by a mechanism that involves the inversion of the CNN or CNC bond angle (ϕ) at one of the nitrogen atoms via a semi-linear transition state.

With respect to the thermal (ground state) isomerization, the three compounds differ significantly in the height of the barrier separating the *cis* (Z) and *trans* (E) isomers. The experimental barrier heights, which are estimated by kinetic measurements, are 176 kJ/mol for stilbene [16], 92 kJ/mol for azobenzene [17] and 70 kJ/mol for NBA [18]. Thus, the thermal barrier between the two isomers of NBA is the lowest and the ground state relaxation from the Z form to the E form is quite rapid, with a rate parameter ca. $1\,s^{-1}$ at room temperature. Hence, the Z isomer can be observed only at low temperatures (ca. 177 K) [19].

Fischer and co-workers [19–21] studied the E–Z isomerization of NBA and of a number of NBA analogs and were able to characterize the thermally labile Z isomers. Subsequently, Asano et al. [22] studied the mechanism of thermal E–Z isomerization of NBA and some substituted NBAs by kinetic studies and quantum chemical calculations at the HF/6-31G* and MP2/3-21G level. They suggest that in the S_0 state the inversion path is favoured with respect to the C=N torsion path. In addition, they distinguish two different inversion paths proceeding via the *planar* ($\alpha = 0°$) and the *perpendicular* ($\alpha = 90°$) orientation of the A ring (see Fig. 1). The theoretical MP2/3-21G value for the *perpendicular* inversion barrier is found to be 68.5 kJ/mol and the *planar* inversion barrier is estimated to be 19 kJ/mol higher [22]. The difference between the perpendicular and planar barrier is attributed to the interaction between the nitrogen lone pair and the aryl π electrons, which is stronger in the perpendicular structure. The calculated MP2/3-21G perpendicular inversion barrier for NBA, 68.5 kJ/mol [22], is quite close to the experimental measure of the barrier height, 70 kJ/mol [18].

Recently, some of the present authors [23,24] have studied the photophysical and photochemical properties of azobenzene. Gagliardi et al. [23] have investigated the low lying excited states of azobenzene to ascertain the role of torsion coordinate in the decay of $S_2(\pi–\pi^*)$ and $S_1(n–\pi^*)$ states. Cembran et al. [24] have investigated the mechanism of Z–E isomerization in azobenzene at the CASPT2 level and have identified the minimum energy path and the conic intersections relevant to the S_1 state. Both the rotational pathway (along the CNNC torsion angle) and the inversion pathway (NNC angle) of azobenzene were studied. It was found [23,24] that isomerization on $S_1(n–\pi*)$ proceeds via the torsion pathway, in contrast with the traditional view favouring the inversion pathway.

In the present paper we reconsider the ground state properties of NBA and begin to study the PES of the lower singlet and triplet states in order to clarify its photophysical and photochemical properties. We start by optimizing the molecular structure and by searching for the more favourable isomerization path in the ground state using density functional (DFT) approach [25–29]. Then, we study the lower excited states energies and their PES along the two possible isomerization coordinates, N=C torsion and the inversion. In this calculation we employ the TDDFT approach [30–32], which is accurate for states based on single excitations, and thus is suitable to study the lowest excited states of NBA. In a study of the excited states of azobenzene [23], the TDDFT approach was found to provide a qualitatively correct picture of the relevant photochemical mechanisms, which was subsequently confirmed by CASSCF/CASPT2 calculations on azobenzene and an azobenzene analog [33] (Conti I, Orlandi G, Rosini G, Garavelli M, to be published). The main purpose of this paper is to assess the role of the inversion (C_7NC_9 angle) and of the rotation ($C_2C_7NC_9$ angle) paths in the Z–E photoisomerization process of NBA excited in the lowest excited states of singlet and triplet spin multiplicity.

2 Computational details

The geometries of the Z and E isomers of NBA were optimized without any symmetry constrains at the DFT/B3LYP [25–29] level of the theory in association with the 6-31G* basis [34]. Vibrational frequencies were evaluated at the DFT/B3LYP level of approximation. For investigations on the alternative isomerization paths we have employed the faster resolution of identity approximation (RI) [35,36] in

Table 1 Most significant geometrical parameters (see Fig. 1) of the S_0 and T_1 equilibrium structures and of the S_0 transition state of NBA, calculated at the DFT/B3LYP/6-31G* level

Structure	θ^a	ϕ^a	α^a	β^a	C_9–N_8^a	N_8–C_7^a	C_7–C_2^a
E-planar	180[b]	123	0	0	1.410	1.282	1.468
E	177	120	39	0	1.406	1.281	1.469
E_{exp}^c			52	0			
Z	4	234	76	13	1.407	1.277	1.483
S_0-TS	3	179	90[d]	0	1.345	1.247	1.486
T_1-opt	94	123	1	8	1.346	1.383	1.420

[a] Bond distances in Å and angles in degree
[b] Constrained value
[c] From ref. [13]
[d] The α' parameter (α is undefined for this structure)

association with the BP86 functional [37,38]. Also the lowest triplet was calculated using the DFT/ B3LYP method.

Turbomole version 5.7 [30–32] was used for the DFT calculations.

3 Results and discussion

3.1 Ground state geometries and vibrational frequencies

The most significant structural parameters, namely the C9–N8, N8–C7 and C7–C2 bond lengths, the θ, α and β torsional angles and the ϕ inversion angle, of the optimized Z and E isomers of NBA in its ground state, are reported in Table 1. The same parameters have been optimized also for the S_0 inversion transition state and for the T_1 equilibrium structure.

For the isomer E, the deviation of the optimized $C_2C_7N_8C_9$ torsion angle (θ), 177°, from the ideal 180° value is tiny (<3°).

The optimized $C_7N_8C_9C_{14}$ torsion angle α by DFT-B3LYP is about 39°. The stabilization energy pertinent to the relaxation of α is only 4.4 kJ/mol. Because of the small energy involved, the torsion around the N_8–C_9 single bond is associated to a low-frequency and large amplitude vibration. It is for this reason that the equilibrium value of α is *strongly dependent on the molecular environment* as noted before [11–15]. Furthermore, its experimental determination, even in the gas phase, is subject to some uncertainty and its theoretical value is bound to depend on the method or level of calculation. The present result for this angle, $\alpha = 39°$, is qualitatively in agreement with the value $\alpha = 45°$ reported in Ref. [11] and with the experimental estimate of 52° obtained by electron diffraction in the gas phase [13].

The Z isomer is found by DFT-B3LYP to be less stable than the E isomer by 26.8 kJ/mol. Because of the steric hindrance between the two benzene rings, the α and β angles are larger than for the E isomer. However, the value of α (76°) is significantly larger than β (13°), in agreement with the very small energy involved in the α twisting of the N–C_9 bond. To our knowledge, the experimental values of the α and β angles of the short-lived Z isomer are not available.

The calculated C_2C_7 and N_8C_9 bond lengths of the central moiety of NBA have similar values in both the E and Z isomers. The lengths of the N_8C_9 (≈1.407 Å) and C_2C_7 (≈1.483 Å) bonds indicate that these are essentially single bonds.

In the lowest S_0 transition structure, which is semi-linear, the C_2C_7 bond keeps the same length, but the N_8C_9 and the C_7N_8 bonds become shorter. In particular, the C_7N_8 bond appears to increase its double bond character.

At variance with S_0, the T_1 optimized geometry is twisted, with $\theta = 94°$, and the values of α and β are small, 1° and 8°, respectively. Thus, the optimized geometry of T_1 coincides with the intermediate between the E and Z isomers along the torsion pathway. As expected, in T_1 the C9–N8 and C7–C2 bonds are shorter while the central N8–C7 bond is longer than in the ground state.

In Table 2 a number of vibrational frequencies of the E isomer, computed at the DFT-B3LYP level, are reported.

The scaled vibrational frequencies of torsion modes are small in agreement with the small energies associated with torsions (vide supra) and in analogy with the corresponding frequencies of stilbene [41–44]. The frequencies involving mainly the N_8–C_9 torsion (α) and the N_8=C_7 torsion (θ), which are associated with highly anharmonic potentials, are 38 and 57 cm^{-1}, respectively. The corresponding experimental values are not available. The computed CN and CC stretching frequencies are in agreement with the available IR and Raman spectra [39,40].

3.2 UV/Vis spectra

The vertical excitation energies of the lowest excited states of the E isomer computed using TD-DFT and DFT methods are presented in Table 3.

Table 2 Selected DFT/B3LYP and experimental frequencies of NBA in the S_0 state

Mode	DFT[a,b]	Expt[b,c][39,40]
$\nu_{CHstretch}$	2906	2885 (w)
$\nu_{CNstretch}$	1638	1633 (vs)
$\nu_{CC(B)stretch}$	1597	1590 (s)
$\nu_{CC(A)stretch}$	1584	
$\nu_{CC(A)stretch}$	1570	1580 (s)
$\nu_{CC(B)stretch}$	1568	
$\nu_{CCNCtorsion}$	57	
$\nu_{CNCCtorsion}$	38	

[a] Frequencies in cm^{-1}
[b] Frequencies are scaled by 0.9608
[c] Legend: w "weak", s "strong", vs "very strong"

Table 3 Vertical excitation energies (eV) of the E-NBA at the DFT and TD-DFT level

State	Excitation energy	
	(TD)-DFT[a]	Exp[b]
S_1	3.74 (0.28)	3.99 (9.0)
S_2	4.49 (0.07)	
S_3	4.58 (0.36)	4.73 (16.7)
S_4	4.65 (0.05)	
(DFT)T_1	2.98[c]	
T_2	3.34	

[a] Oscillator strengths are in brackets
[b] From ref. [8]; extinction coefficients/10^3 are in brackets
[c] DFT value

The calculated excitation energies of S_1 and S_3 singlet states are in qualitative agreement with the experimental values [8], although they appear to underestimate the excitation energies by ca. 0.2 eV. However, it is worth noting that the experimental data are not clear-cut since they are derived from low-resolution absorption spectra measured in solution. The calculated oscillator strength of S_2 and S_4 are relatively small and this may explain the lack of these states in the assignment of the absorption spectrum.

For the T_1 and T_2 triplet states of NBA, the DFT and TD-DFT vertical excitation energies are 2.98 (287 kJ/mol) and 3.34 eV (322 kJ/mol), respectively. To the best of our knowledge, there are no $S_0 \rightarrow T_i$ absorption spectra in the literature giving the vertical excitations. The only experimental information available pertains to the T_1 equilibrium energy and is obtained by measuring the rate constants of the NBA triplet quenching by a number of compounds of known triplet energy. The T_1 energy of NBA obtained in this way is about 230 kJ/mol or 2.38 eV [45]. Since the difference between vertical and equilibrium energies is about 0.5 eV in normal hydrocarbons, we believe that the DFT result represents a qualitatively good estimate of the T_1 energy.

3.3 Potential energy curves

The DFT/B3LYP potential energy curves along the inversion and torsion (ϕ and θ) coordinates have been calculated by the constrained optimization technique. These results, reported in the subsections below, will shed some light on the pathways of the isomerization and photoisomerization process in NBA.

3.3.1 The inversion pathway

The inversion curves for S_0 and T_1 states were computed by constraining the ϕ angle (CNC) to fixed values and relaxing all other degrees of freedom. The curves are presented in Fig. 2.

It can be seen that the semi-linear structure ($\phi = 180°$) has a maximum in both S_0 and T_1 energy curves. Starting from these structures we searched for the transition state (TS) and E and Z isomer minimum structures. It was found that both singlet and triplet transition state structures are practically semi-linear ($\phi = 179°$). Nevertheless, the values of the α' dihedral angle differ significantly (89° for S_0, 67° for T_1). Furthermore, the Z and E structures in T_1 do not correspond to minima on the potential energy surface as discussed below in the torsion pathway section. The most significant geometrical parameters of the semi-linear TS structures are reported in Table 4.

From the DFT energies of E (0 kJ/mol) and Z (26.8 kJ/mol) isomers in S_0 and of the transition state (83.8 kJ) we find that the activation barrier of the Z–E isomerization via the inversion pathway is equal to 57 kJ/mol, a value somewhat lower than the energy found by Asano et al. [22] (68.5 kJ/mol) with a MP2/3-21G calculation and than the experimental estimate (70 kJ/mol) [18]. Considering the level of the calculation (HF-MP2/3-21G), the agreement between theory and experiment is noteworthy.

The barrier on the T_1 curve is very high and thus it prevents the photoisomerization on T_1 to occur along the inversion pathway.

3.3.2 The rotational pathway

The alternative rotational isomerization pathway of the S_0 and T_1 states was constructed as a series of constrained optimization keeping the CCNC torsion angle (θ) at fixed values. The resulting energy curves are displayed in Fig. 3.

In the case of S_0 we observe that, as the dihedral angle θ approaches 90°, the optimized value of ϕ becomes 180°, that is, the molecular structure becomes semi-linear. Precisely, in the interval $\theta = 65°, \ldots, 115°$ the starting structures

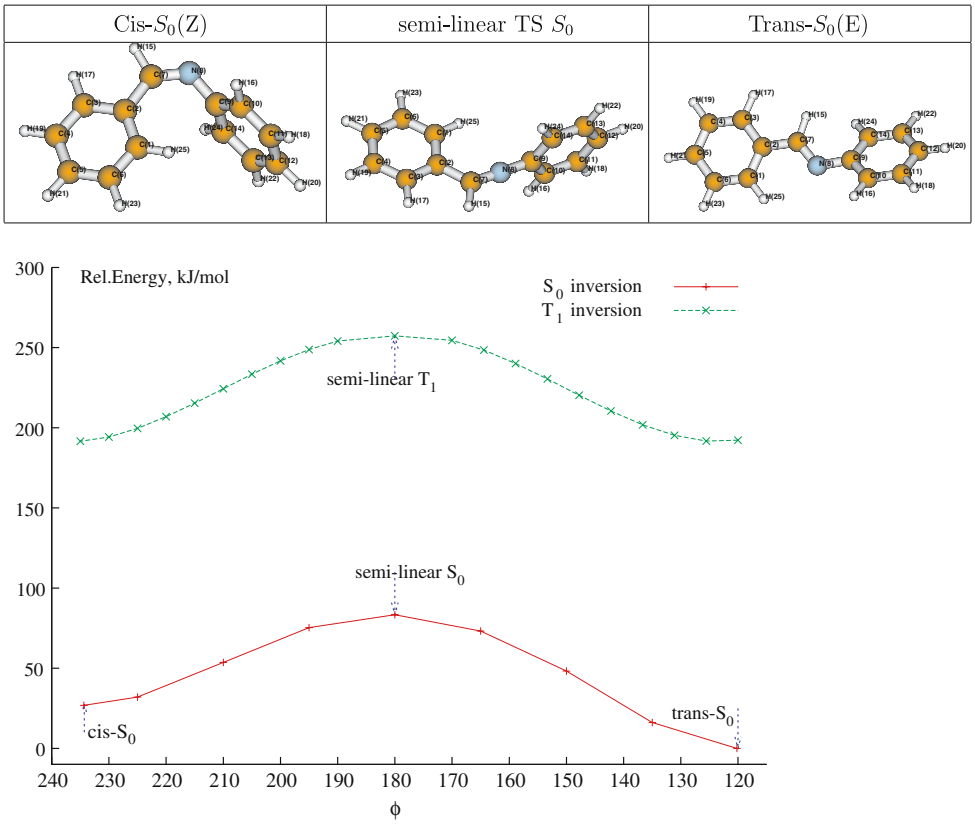

Fig. 2 DFT S_0 and T_1 optimized potential energy curves for the inversion coordinate

Table 4 DFT optimized energies (kJ/mol) and significant ϕ, α' and β geometrical parameters (see Fig. 1) of E, Z and transition state structures along the inversion and torsion pathways in S_0 and T_1

Structure	θ^a	ϕ^a	$\alpha^a(\alpha')^a$	β^a	ΔE
S_0 E isomer	177	120	39	0	0.0
S_0 Z isomer	4	234	76	13	26.8
S_0 semi-linear TS	–	179	(89)	0.3	83.8
S_0 twisted structure	90	180	12	7	154
T_1 E isomer[b]					287
T_1 Z isomer[b]					324
T_1 semi-linear TS	–	179	(67)	2	257
T_1 torsional TS	94	123	67	8	191

[a] Angles in degrees
[b] Vertical energy

converge to the same semi-linear geometry ($\phi = 180°$), which is 83.8 kJ/mol above the E structure. The pure rotational pathway for the isomerization has to overcome a much higher barrier (154 kJ/mol, see below). Therefore, in the S_0 state the molecule will not follow this pathway.

A different picture is observed for the case of the triplet state T_1. Unconstrained energy minimization gives a twisted structure without any significant increase of the ϕ angle, in which $\theta = 94°$ and $\phi = 123°$. It is interesting to note that for $\theta < 30°$, close to the Z structure, the T_1 optimization gives a semi-linear structure. The T_1 energy minimum at the twisted geometry is 192 kJ/mol while the vertical triplet excitation energy of the E structure is 288 kJ/mol. These values bracket the experimental energy of T_1, 230 kJ/mol [45].

3.3.3 Potential energy surface of the isomerization process

To further clarify the features E–Z isomerization, we have calculated the ground state potential energy surface of NBA along the C=N torsion (θ) and the CNC inversion (ϕ)

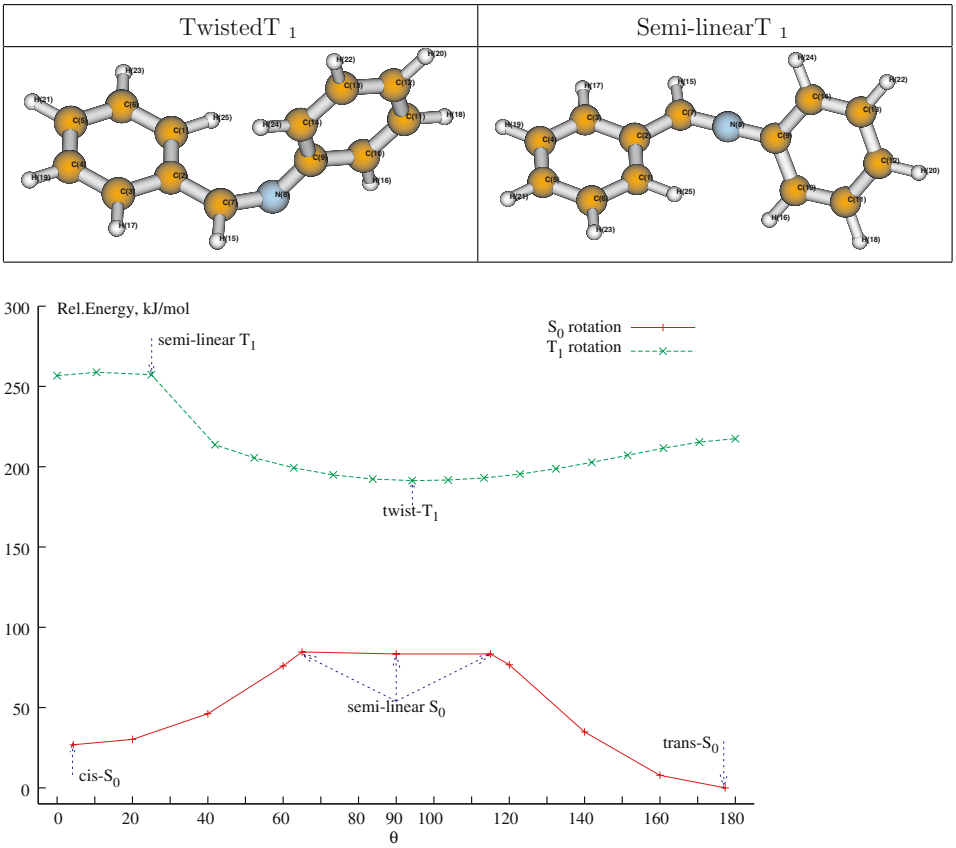

Fig. 3 DFT optimized S_0 and T_1 potential energy curves for the C=N torsion coordinates

coordinates. The results are shown in Fig. 4. The coordinates explored are in the range $0° \leq \theta \leq 180°$ and $120° \leq \phi \leq 240°$. At each point of the θ and ϕ surface, all other geometry parameters were optimized using the DFT-RI/BP86/6-31G* method.

The pure inversion path in S_0 corresponds approximately to the line connecting the Z and E isomers parallel to the ϕ axis and the pure rotational path corresponds to the line connecting the Z and E parallel to θ axis.

We see that pure inversion path crosses the iso-line corresponding to the semi-linear structure and is stable with respect to the optimization of the torsion coordinate. On the other end, the pure rotational path in S_0 encounters a very high barrier about 154kJ/mol, above the inversion transition state (83.8 kJ). This barrier corresponds to the breaking of the C=Nπ bond and to a biradicalic electronic structure: for this reason its sharp energy is probably overestimated by the DFT calculation (see for example the DFT calculation on azobenzene [23]). The attempt to minimize the energy keeping $\theta = 90°$ changes ϕ and leads the molecule to the semi-linear structure. Thus, even if the molecule may initially move along the rotation path at some stage it will switch to the inversion path.

While the high barrier found rules out the torsion mechanism in the S_0 state, it contributes to the decrease of the T_1–S_0 energy gap and tends to shorten the T_1 lifetime for the energy gap law of radiationless transitions. This is in agreement with the experimental measure of $\tau(T_1)$ that indicates a quite short lifetime of <0.05 μs [43].

Asano et al. [22] have suggested that E–Z inversion pathway is possible through planar and perpendicular transition states. These two transition structures differ by the value of the dihedral angle α' . To investigate this aspect we have studied the potential energy surface in the (α', ϕ) coordinate space and the results are shown in Fig. 5. The surface was constructed with DFT-RI/BP86/6-31G* method. Minima and saddle points were further optimized using DFT/B3-LYP/6-31G* method and vibrational analysis was performed to verify that the number of imaginary frequencies is correct.

We see from Fig. 5 that there is only one transition state (TS_1) possible between the Z and E isomer, and this corresponds to the perpendicular structure ($\alpha' = 90°$). Its geometrical parameters and energy correspond to those of the TS structure found on the inversion isomerization pathway. The structure corresponding to $\alpha' = 0°$ is a maximum in

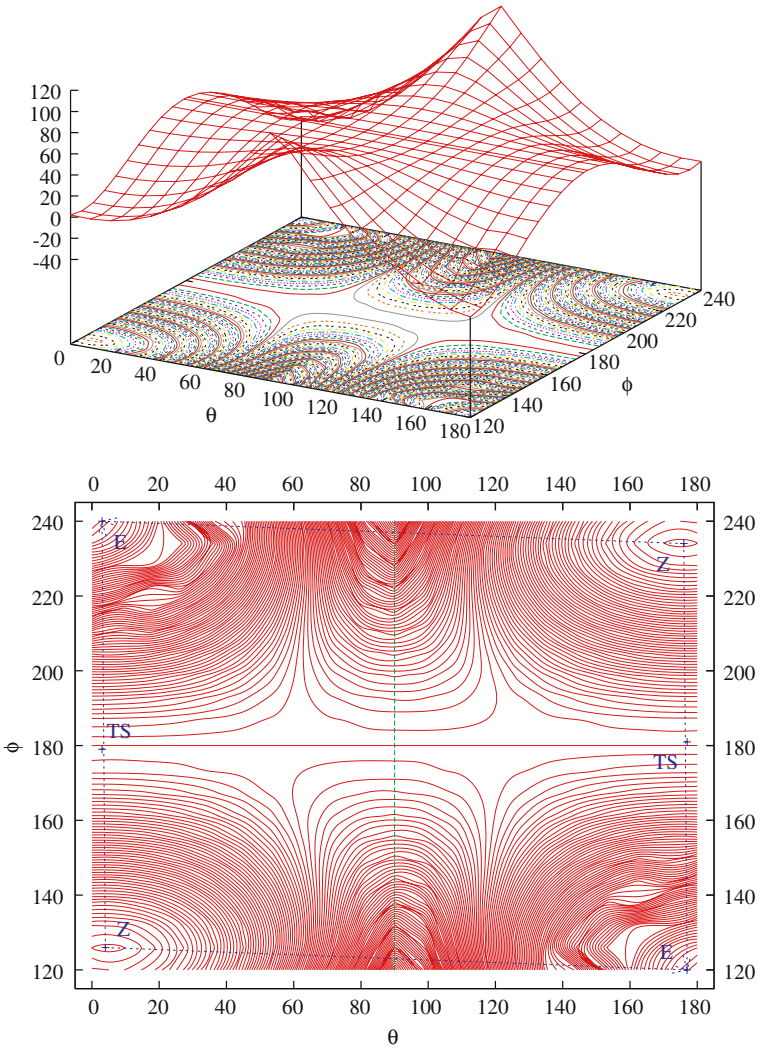

Fig. 4 DFT ground state potential energy curve along the θ and ϕ coordinates

this coordinate space. The two E-structures "E-1" and "E-2" have the same energy and are connected by a 180° rotation of the A-ring via the TS_2 transition state.

3.3.4 Role of excited states in the inversion pathway: TDDFT potential energy curves

To study the feasibility of photoisomerization of NBA in excited states, we have computed the potential energy curves (PECs) of the lowest excited states along the inversion pathway, which are obtained by adding the appropriate TD-DFT vertical excitation energies to the optimized DFT ground state energies. Therefore, these PECs are not optimized with respect to energy and can have only a qualitative meaning. In Fig. 6 we report the PECs of the ground state and the two lowest excited triplet and singlet states.

It can be noted that the energy of the T_1 PEC is much higher than the ground state PEC in agreement with the optimized PECs obtained by DFT and as shown in Fig 2. This rules out the possibility that thermal isomerization can occur via the lowest triplet, as found for azobenzene [23,24]. The non-optimized TD-DFT curve is practically flat. Its qualitative character by itself cannot give clear indication about the possibility of isomerization in this state. However, the optimized T_1 PEC obtained by DFT shows a barrier at the inverted structure (see Fig. 2) and thus the photoisomerization in T_1 is very unlikely to occur via inversion. This process, as discussed above, takes place in T_1 along the torsion coordinate.

The PEC of S_1 has a minimum for the semi-linear geometry and, therefore, we expect that both the E–Z and Z–E photoisomerizations are feasible with appreciable yields. This agrees with experimental findings [19], which show that the photoprocess occurs even at temperatures as low as 173 K.

More quantitative statements about quantum yields and excited state lifetimes would require consideration of the

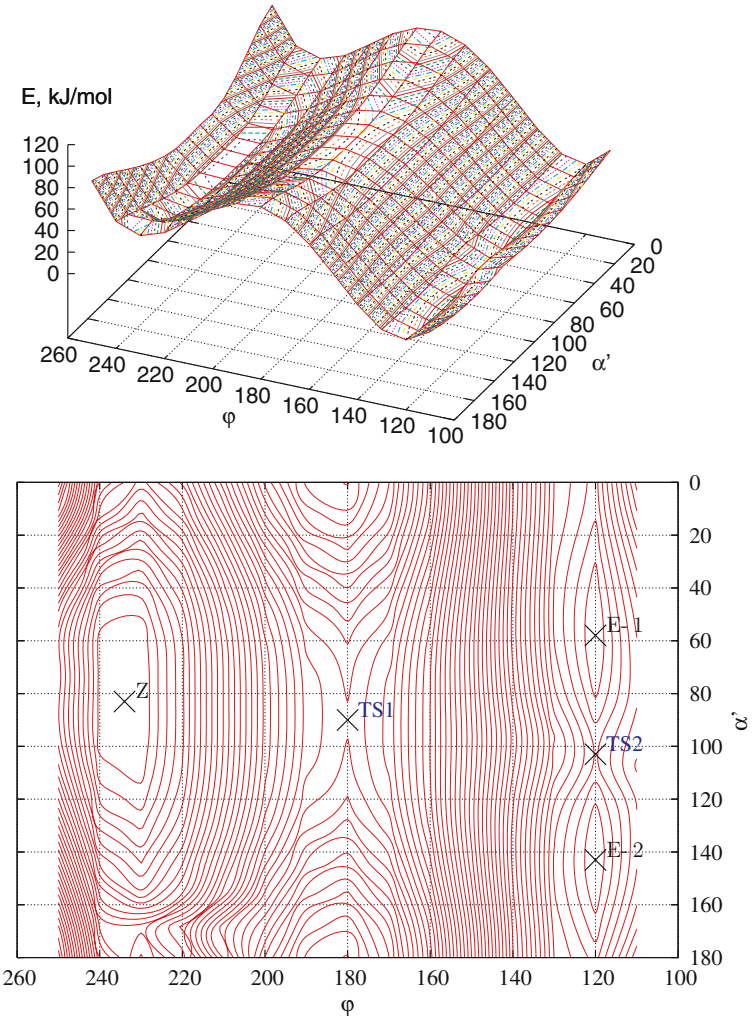

Fig. 5 Ground state potential energy surface along the α' and ϕ coordinates

minimum energy paths on the hyper-PES of each electronic state of interest and the calculation of multiconfiguration wavefunctions. Such calculations are currently under way to complement and extend the present results.

4 Conclusions

In this work we have presented the results of preliminary calculations of the properties of NBA isomers and of their thermal and photochemical inter-conversion. The main conclusions are as follows:

– The E-isomer of NBA has a non-planar structure, with the N-ring α angle of ca. 40°, in agreement with previous work [11]. It is more stable than Z-isomer by 27 kJ/mol according to DFT approach, in agreement with the very low equilibrium ratio between the concentrations of the Z and E isomers: [Z]/[E] < 1% [19]. For this reason, it is difficult to characterize the Z form.

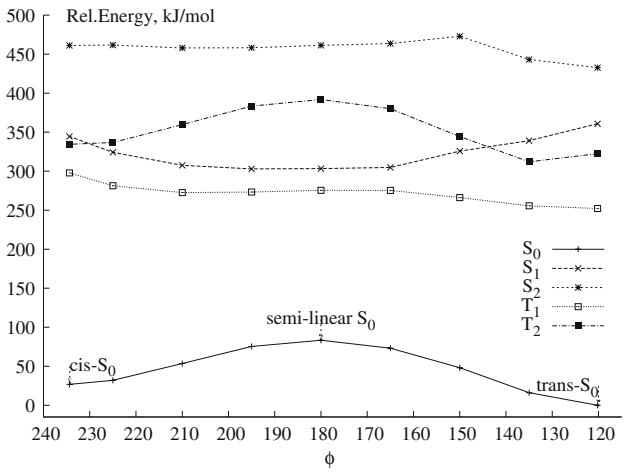

Fig. 6 TDDFT potential energy curves along the inversion coordinate for the lowest singlet and triplet states

– The DFT potential energy surface on θ and ϕ coordinates suggests that the CNC inversion is the preferred path for the Z–E ground state isomerization, in agreement with a

previous study [22]. The optimized semi-linear TS along the inversion path shows a perpendicular phenyl and its calculated energy is 57 kJ/mol above the isomer Z, by the DFT calculation, in qualitative agreement with the experimental estimate (70 kJ/mol)[18].

– The DFT T_1 potential energy curves along the θ and the ϕ coordinates indicate that inversion is not the preferred path for the Z–E sensitized photo-isomerization in this state. This process appears to be very favoured along the torsion (θ) coordinate, because the T_1 PEC has a rather deep minimum for $\theta = 90°$. This result is confirmed by the observation of sensitized photo-isomerization down to 200 K [19].
– The potential energy curves of the lowest excited singlet states along the inversion path have been calculated by the TDDFT method. The main finding concerns the S_1 PEC, which shows a minimum for $\phi = 180°$. This result suggests that the E–Z photoisomerization in S_1 is feasible, in agreement with the observations performed by Maeda and Fischer [19] down to the temperature of 173 K.

Acknowledgments Authors would like to thank the Lunarc computational facility at Lund University for the computational support. G. O. is grateful to MURST PRIN 2005 (project: "Trasferimenti di energia e di carica a livello molecolare") for financial support. L.G. thanks the Swiss National Foundation, grant N.200021-111645/1.

References

1. Henderson R, Baldwind JM, Ceska TA, Zemline F, Beckmann E, Downing K (1990) J Mol Biol 213:899
2. El-Sayed MA (1992) Acc Chem Res 25:279
3. Singh AK, Majumdar N (1994) Photochem Photobiol 60:510
4. Padwa A (1977) Chem Rev 77:1
5. van Walree CA, Franssen O, Marsman AW, Flipse MC, Jenneskens LW (1997) J Chem Soc Perkin Trans 2:799
6. Brocklehurst P (1962) Tetrahedron 18:299
7. Haselbach E, Heilbronner E (1968) Helv Chim Acta 16:16
8. El-Bayoumi MA, El-Asser M, Abdel-Halim F (1971) J Am Chem Soc 93:586
9. Burgi HB, Dunitz JD (1970) Helv Chim Acta 52:1747
10. Akaba R, Tokumaru K, Kobayashi T (1980) Bull Chem Soc Jpn 53:1993
11. Bernstein J, Engel YM, Hagler AT (1981) J Chem Phys 75:2346
12. Patnaik LN, Das S (1985) Int J Quantum Chem 27:135
13. Traetterber M, Hilmo I, Abraham RJ, Ljunggren S (1978) J Mol Struct 48:395
14. Gill VMS, Saraiva MEL (1971) Tetrahedron 27:1309
15. Bernstein J, Schmidt GMJ (1972) J Chem Soc Perkin Trans 951
16. Kistiakowsky GB, Smith WR (1934) J Am Chem Soc 56(3): 638–642
17. Brown EV, Granneman GR (1975) J Am Chem Soc 97(3): 621–627
18. Geibel K, Grellmann K, Staudinger B, Wendt H (1972) Ber Bunsenges Phys Chem 76:1246
19. Maeda K, Fischer E (1977) Israel J Chem 16:294
20. Fischer E (1967) J Phys Chem 71:3704
21. Fischer E, Frei Y (1957) J Chem Phys 27:808
22. Asano T, Furutaa H, Hoffmann H-J, Cimiraglia R, Tsuno Y, Fujio M (1993) J Org Chem 58:4418–4423
23. Gagliardi L, Orlandi G, Bernardi F, Cembran A, Garavelli M (2004) Theor Chem Acta 111:363–372
24. Cembran A, Bernardi F, Garavelli M, Gagliardi L, Orlandi G (2004) J Am Chem Soc 126:3234
25. Lee C, Yang W, Parr RG (1988) Phys Rev B 37(2):785–789
26. Becke AD (1988) Phys Rev A 38(6):3098–3100
27. Dirac PAM (1929) Proc R Soc (London) A 123:714
28. Slater JC (1951) Phys Rev 81:385–390
29. Vosko S, Wilk L, Nussair M (1980) Can J Phys 58:1200
30. Treutler O, Ahlrichs R (1995) J Chem Phys 102(1):346–354
31. Furche F, Ahlrichs R (2002) J Chem Phys 117(16):7433–7447
32. Bauernschmitt R, Ahlrichs R (1996) Chem Phys Lett 256(4–5): 454–464
33. Conti I, Marchioni F, Credi A, Orlandi G, Rosini G, Garavelli M (2007) J Am Chem Soc 129:3198–3210
34. Hariharan PC, Pople JA (1973) Theor Chim Acta 28(3):213–222
35. Eichkorn K, Treutler O, Öhm H, Häser M, Ahlrichs R (1995) Chem Phys Lett 240(4):283–289
36. Eichkorn K, Weigend F, Treutler O, Ahlrichs R (1997) Theor Chem Acc 119(1–4):119–124
37. Perdew JP (1988) Phys Rev B 33(2):8822–8824
38. Becke AD (1986) J Chem Phys 84:4524
39. Meic Z, Baranovic G (1989) Pure Appl Chem 61(12):2129–2138
40. Kozhevina LI, Prokopenko EB, Rybachenko1 VI, Titov EV (1995) J Appl Spectrosc 59(5–6):805–809
41. Suzuki T, Mikami N, Ito M (1986) J Phys Chem 90:6431
42. Spangler LH, van Zee R, Zwier TS (1987) J Phys Chem 91:2782
43. Chiang WY, Laane J (1994) J Chem Phys 100:8755
44. Gagliardi L, Orlandi G, Molina V, Malmqvist PA, Roos B (2002) J Phys Chem A 106:7355
45. Görner H, Fischer E (1991) J Photochem Photobiol A Chem 57:235